J. Biomechanics Vol. 23, No. 8, pp. 763–771, 1990.
Printed in Great Britain

0021-9290/90 $3.00 + .00
Pergamon Press plc

THE BENDING PROPERTIES OF SINGLE OSTEONS

A. ASCENZI, P. BASCHIERI and A. BENVENUTI

University of Rome 'La Sapienza', Department of Bio-pathology, Policlinico 'Umberto I', Viale Regina Elena 324, I-00161 Rome, Italy

Abstract—The bending properties of two fully calcified osteon types (longitudinal and alternate) have been investigated in 62 cylindrical samples by applying the technique of three-point bending loading. The bending of each sample was recorded using a microwave micrometer based on the cavity and pulse technique. It has been shown that alternate osteons are better able to withstand bending stress than longitudinal ones.

This result offers a definitive explanation for the high concentration of transverse lamellae in pathologically bowed bone shaft.

INTRODUCTION

Tensile, compressive and shearing stresses are the components of bending stress, and all are affected by the cross-sectional area of the specimen. None of them, however, does this uniformly so it is hard to calculate the magnitude of the various kinds of components and the relative contribution of each to the failure mechanism. As a result, bending has generally been considered an unreliable way of investigating the mechanical properties of a material (Evans, 1973).

Despite this, over the last hundred years or so, experimental investigations on the properties of human whole bone structures in a bending loading configuration have been performed by several authors: Messerer (1880), Knese *et al.* (1956), Motoshima (1960), Stevens and Ray (1962), Mather (1968), Ehler and Lösche (1970), Azang *et al.* (1972), Martens *et al.* (1986). Moreover, standardized specimens of cortical bone have been tested in bending by Rauber (1876), Maj and Toajari (1937), Olivo (1937), Olivo *et al.* (1937), Maj (1938 a,b), Toajari (1938), Sedlin (1965), and some Japanese researchers, as reported by Yamada (1970). Each of these investigations partly arose out of the need to study the mechanism of bone fractures which are often produced by bending stresses, and were partly undertaken to explore the relationship between the macroscopic and the microscopic mechanical properties of bone.

So far no systematic investigations on the bending properties of single osteons have been carried out, so we recently began a study to obtain information on this subject. After some very preliminary data had shown that alternate osteons reveal some differences in behaviour with respect to longitudinal osteons when loaded by bending (Ascenzi *et al.*, 1987), we decided to find out whether this result would be confirmed by a large-scale quantitative investigation which is now reported in the present paper.

Received in final form 9 *November* 1989.

MATERIALS AND METHODS

When fully formed, the osteon is an irregularly cylindrical and branching structure a few millimeters long, showing many transverse canals (known as Volkmann's canals) originating from the central Haversian canal. A cross-section, no thicker than 500 μm, from the diaphysis of a long bone, usually contains the straight non-branching portions of many osteons and fails to reveal any Volkmann's canals. If these portions could be cut out from a bone section, they would be suitable samples for testing by bending.

Working on this principle, cross-sections of femoral human shafts measuring 500 μm in thickness were prepared using a 'Leitz 1600' microtome equipped with a rotating saw. A thickness of 500 μm is a critical limit beyond which a bone section is no longer sufficiently transparent for examination under the polarizing microscope, although bone transparency may be increased to some extent by soaking the section in bromoform. The structure of each osteon was accurately checked by examining thin sections from each unit after testing.

The osteon samples were obtained from bone cross-sections using a previously described, specially designed device (Ascenzi and Bonucci, 1968). This consisted of a very thin, carefully sharpened steel needle which had been eccentrically inserted on a dentist's drill. While the drill was turning, the tip of the needle described a circle whose diameter corresponded to the average diameter of an osteon. If the rotating axis of the needle coincided with the axis of an osteon, and this was oriented at right angles to the surfaces of a bone section, the tip of the needle could rotate just inside the osteon's limits, cutting out an osteon sample which had the shape of a cylinder with a wall of almost uniform thickness.

To ensure that the rotating needle was perpendicular to the bone section, the hand-piece of the drill was inserted into the body of a microscope from which the tube had previously been removed and the section was firmly fixed onto the stage. By coarse adjustment of

the microscope it was easy to regulate the movement of the needle into the bone section. The cutting of the osteon was controlled by watching the operation with a steroscopic microscope.

In applying the technique described here, special attention was paid to ensure that the following main requisites would be accurately fulfilled. Firstly, in all the osteons that were chosen, the haversian canal was aligned with the long axis of the cylindrical sample. Secondly, a careful check was made that the external diameter (D) of each isolated sample measured 195 μm with a tolerance of 3 μm. Finally, as regards the diameter of the haversian canal (d), two series of samples were selected, those measuring 40 μm and those measuring 50 μm, respectively, both with a tolerance of 3 μm. The reason for the selection of two series of units is that it is very difficult to find osteons which all have a haversian canal with the same diameter. So the selection of two series of units had the aim of seeing whether the results of two different experiments would be mutually validating.

All the tested osteons showed the same degree of calcification, but the orientation of their collagen bundles differed. The degree of calcification was determined microradiographically, the aim being to select fully calcified units. This was done by applying the criteria and the method reported in previous papers (Ascenzi and Bonucci, 1967, 1968; Ascenzi, 1983). Among the different arrangements produced by differences in fiber bundle direction in successive lamellae, those characteristic of two types of osteons were chosen. In the first type (called 'alternate' here) the fibers in one lamella have a marked longitudinal spiral course, while in the next the fibers have an almost transversal spiral course so that the fibers in two successive lamellae make an angle of nearly 90°. Under the polarizing microscope, the osteons of this type reveal an alternation of dark and bright lamellae in cross-section. In the second type (called 'longitudinal' here) the fibers have a marked longitudinal spiral course with the pitch of the spiral changing so slightly that the angle of the fibers in one lamella is practically the same as that of the fibers in the next. Under the polarizing microscope, the osteons belonging to this type appear dark in cross-section; they are often bordered by a few bright lamellae. Moreover, from the dark background thin bright curved lines stand out concentrically round the haversian canal. These lines are short and irregularly distributed, so that they never reveal a complete annular arrangement. They are commonly interpreted as sketchings of transverse lamellae (Ascenzi and Bonucci, 1976).

In selecting these two types of osteons, some particular structural features concerning the orientation of fiber bundles in alternate osteons (Ascenzi and Benvenuti, 1986; Giraud-Guille, 1988) were disregarded here.

The samples were subjected to bending strength by using the device illustrated in Fig. 1(a). Each osteon measuring 500 μm in length was freely supported at both ends by the edges of two tiny steel plates situated on exactly the same horizontal plane. Since the distance between the edges was 400 μm, the last 50 μm of the osteon sample, at each of its ends, lay on a steel plate. In this way the angular rotation of the ends of the osteon at the supports was not impeded as the osteon bent under the load. The osteon was made to bend by loading the central part of the sample using a steel point whose contact surface measured 80 μm along the osteon axis and 250 μm at right angles to that axis. Owing to the shortness of the specimen, a surface of this kind reduced artificial deformations to a minimum, even if it could not completely avoid them. This residual problem does not, however, seem to have significantly affected the results of the present investigation. The steel point was attached to a cylinder that contained a horizontal beam and could move freely inside a vertically oriented cavity. A thin nylon thread was fixed to the two ends of the beam and a series of loads each weighing 12 g were attached to it (Fig. 2). The total weight of the steel point, the cylinder with its horizontal beam and the nylon thread was 5.8 g. The forward movement of the steel point that bent the osteon sample was recorded by a specially devised microwave micrometer described below. As soon as the bending of an osteon produced by the addition of a load became constant, additional weights were added. Difficulties were encountered in applying this method when the stress had passed the elastic limit. In this case, it was hard to decide when a new equilibrium had been reached. In practice, therefore, more weights were added when the speed of elongation produced by each successive increase in stress had slackened considerably.

Particular attention was paid to reducing to a minimum any longitudinal or rotational displacement of the sample with respect to the steel point during loading. All the measurements were performed at a temperature of about 20°C.

The material used in the present investigation was obtained from femoral shafts of human subjects aged between 19 and 36—shafts apparently free from skeletal defects. The total number of prepared osteon samples was 485, of which 423 were discarded because they did not strictly satisfy the conditions reported above. So, only 62 samples were loaded in bending. Of these samples 37 (21 longitudinal and 16 alternate) had haversian canals measuring 40 μm in diameter, and 25 (14 longitudinal and 11 alternate) had haversian canals measuring 50 μm in diameter.

The wet osteons were obtained by hydration of the material using saline solution.

In measuring the changes in the forward movement of the steel point for osteons subjected to bending stress, a microwave micrometer based on the cavity and pulse technique was used. The principle on which it works is the same as that of the extensimeter and the pressimeter described in previous papers (Ascenzi *et al.*, 1966; Ascenzi and Bonucci, 1967, 1968; Ascenzi *et al.*, 1985).

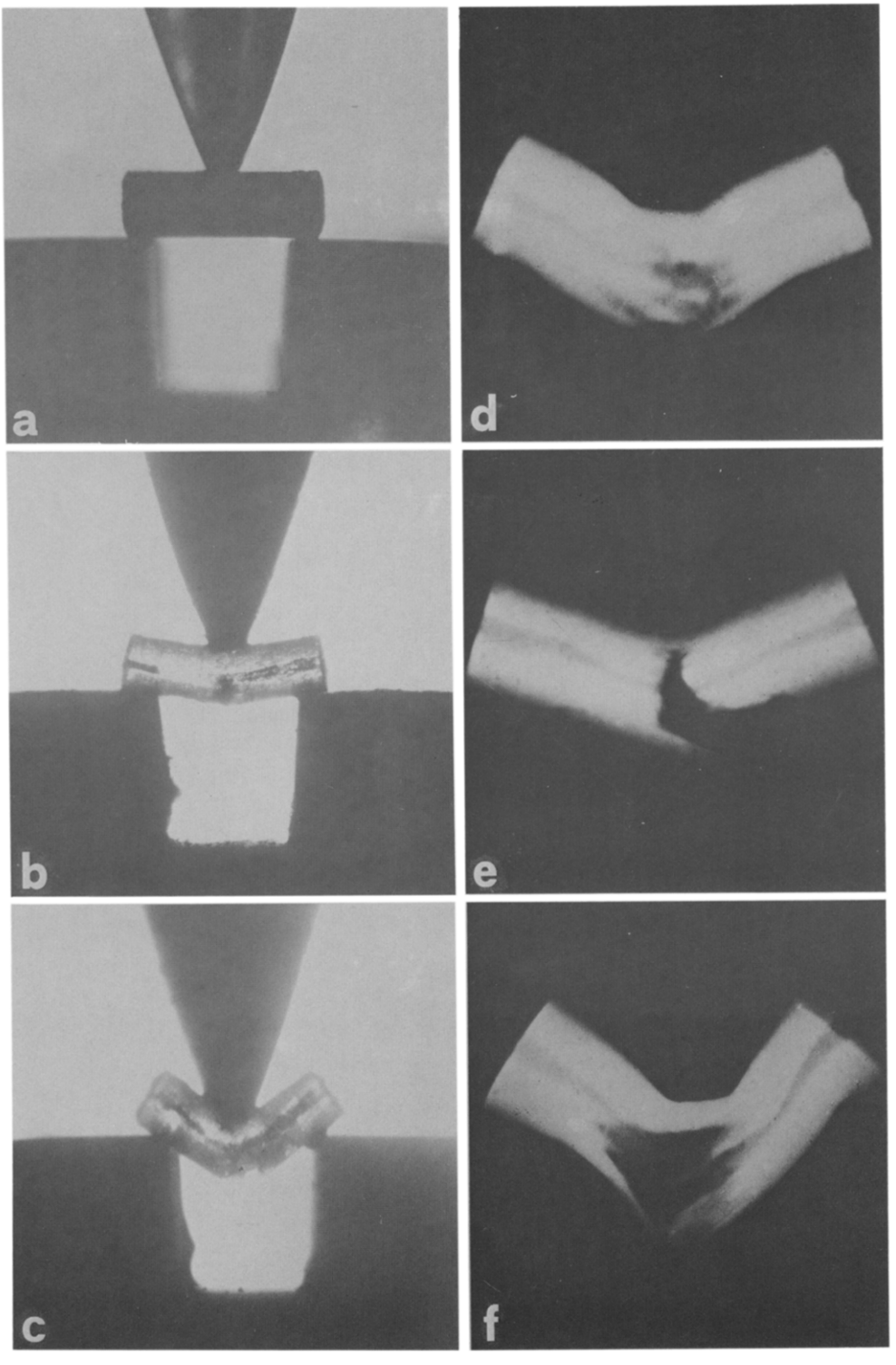

Fig. 1. (a) Cylindrical osteon sample ready to be bent; (b) alternate osteon sample at ultimate bending strength; (c) longitudinal osteon sample at ultimate bending strength; (d) microradiograph of a fractured longitudinal osteon sample; (e) microradiograph of a fractured alternate osteon sample; (f) microradiograph of an irregular type of fracture in an alternate osteon sample.

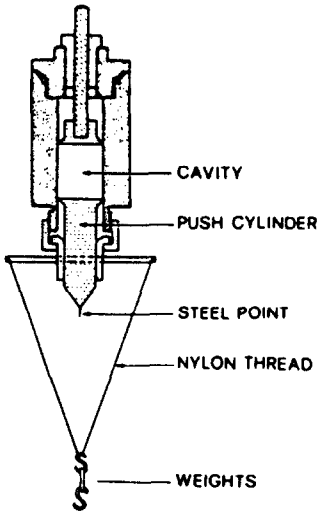

Fig. 2. Diagram of the cavity used for recording the deformation of an osteon loaded by bending.

Figure 2 presents a diagram of the cavity used for measuring the deformation of the osteon specimens submitted to bending stress. The steel point is fixed to the push cylinder whose upper surface is the lower plane of a cylindrical cavity, which functions as a resonator for electromagnetic waves. When weights are attached to the push cylinder, the osteon sample undergoes a deformation in bending which makes the lower plane of the cylindrical cavity fall, so increasing the height of the cavity. As the deformation of the sample is exactly equal to the elongation in the height of the cavity, changes in the bending of the sample are easily deduced from changes in the resonant frequency of the cavity.

Measurement of changes in bending for a single sample were accurate to within 1%. Greater accuracy was unnecessary because the geometrical dimensions of the osteon samples could not be measured more accurately than that.

To investigate the histological changes produced by bending stress in isolated osteons, these last were submitted after fracture to microscopic and microradiographic examination without any previous treatment.

In concluding this section, it appears worth pointing out that the shape of the osteonic specimen is unusual for a proper bending test, the length resulting necessarily reduced in respect to the external diameter. So, a large shearing stress exists at the failure site. However, this occurrence seems negligible because the aim of the present investigation is not to furnish absolute data, but only to study the behaviour in bending of two different osteon types.

RESULTS

Under microscopic examination, different kinds of fully calcified osteon samples loaded by bending behaved in quite different ways, depending upon the orientation of collagen fibers and crystallites in successive lamellae. Longitudinal osteons, that is, osteons whose fibers have a marked longitudinal spiral course in successive lamellae, show conspicuous deformation before fracture occurs. On the other hand, alternate osteons, that is, osteons in which the fibers in one lamella have a marked longitudinal spiral course, while those in the next have an almost transverse spiral course, show relatively little deformation before fracture occurs. Direct evidence about these findings may be obtained by examining Fig. 1(b) and (c). The former shows a bent alternate osteon and the latter a bent longitudinal osteon when failure had been reached.

The difference between the bending of the two osteon types appears even more obvious when the bending diagrams are examined. In Fig. 3 six typical diagrams are shown, three (a, b, c) corresponding to alternate osteons, and the others (d, e, f) to longitudinal osteons; all these osteons had a haversian canal averaging 40 μm in diameter. The diagrams obtained from the alternate and longitudinal osteons that had an inner diameter of 50 μm resemble those shown in Fig. 3, so no examples of this type have been given. The alternate osteons of the two series are characterized by a curve which approximates to a straight line almost as far as fracture, indicating a proportionality of stress and strain in line with Hooke's law. Only the uppermost points show a portion of deviating curve before the sample breaks.

On the other hand in the diagrams recorded from the longitudinal osteons of the two series, the curve initially approximates to a straight line, as with the diagrams obtained from alternate osteons. But as the bending of the sample increases towards breaking point, a change of slope occurs corresponding to elasto-plastic deformation. This portion does not last long, however; the curve straightens out again, resuming its upward slope, and after a certain distance fracture occurs.

The experimental numerical data obtained from each tested osteon are reported in Tables 1 and 2. They are: the ultimate bending load (UBL), the ultimate bending deformation (UBD), the elastic modulus E1 (calculated for a load of 0.58 N), the elastic modulus E2 (calculated for a load of 1.99 N) and the modulus of rupture (MOR). In line with the beam theory, E1, E2 and MOR were calculated by applying the following equations:

$$E = \frac{P}{\Delta}\frac{L^3}{48I} \qquad \mathrm{MOR} = \frac{P \cdot L/4 \cdot D/2}{I}$$

where P is the load, Δ the deformation, L the osteon length and I the moment of inertia. This last is given from the formula $\pi/64\,(D^4 - d^4)$, where D and d are the external and internal diameter of the osteon.

The mean values reported in Tables 1 and 2 for UBL, UBD, E1, E2 and MOR have been statistically

Table 1. UBL (in N), UBD (in μm), E (in GPa) and MOR (in GPa) for alternate and longitudinal osteons whose haversian canal was 40 μm in diameter. E was calculated for loads of 0.58 N (E1) and 1.99 N (E2), respectively

	Alternate osteons					Longitudinal osteons				
	UBL	UBD	E1	E2	MOR	UBSg	UBSn	E1	E2	MOR
	1.99	66.5	1.58	0.56	0.27	2.23	87.5	1.16	1.05	0.30
	2.23	69.0	4.42	0.83	0.30	2.94	118.0	1.47	0.87	0.40
	2.46	84.0	3.16	0.97	0.33	3.17	104.5	2.21	1.39	0.43
	3.17	90.1	2.42	1.73	0.43	2.82	111.0	1.10	0.83	0.38
	2.11	85.5	4.42	0.51	0.29	2.11	132.0	3.68	0.34	0.29
	2.58	64.5	1.38	1.25	0.35	3.29	104.0	3.68	0.96	0.45
	2.11	52.5	2.21	0.86	0.29	3.17	144.5	1.00	0.49	0.43
	2.70	44.0	3.68	2.68	0.37	3.64	174.5	2.45	0.94	0.50
	2.94	51.5	2.76	2.03	0.40	2.58	144.0	1.49	0.44	0.35
	2.46	72.0	2.01	0.64	0.33	2.58	139.0	1.00	0.35	0.35
	2.94	45.5	2.76	3.13	0.40	3.05	126.5	1.61	0.69	0.41
	2.46	34.0	3.68	2.35	0.33	2.70	141.3	2.15	0.34	0.37
	2.82	51.5	2.45	2.09	0.38	3.17	197.0	3.23	0.42	0.43
	3.05	86.0	2.21	1.71	0.41	2.82	201.0	1.38	0.48	0.38
	3.17	75.0	2.21	1.88	0.43	2.23	159.0	2.45	0.32	0.33
	2.70	84.0	1.84	1.25	0.37	3.29	140.5	4.42	1.47	0.60
						3.64	128.5	2.76	0.99	0.37
						3.41	99.5	1.70	1.41	0.46
						3.52	106.5	4.42	2.21	0.48
						2.35	122.0	1.10	0.46	0.32
						2.46	107.0	4.42	0.55	0.33
Mean	2.61	66.01	2.69	1.53	0.355	2.91	132.75	2.32	0.809	0.398
S.D.	0.38	17.65	0.93	0.79	0.051	0.47	30.53	1.20	0.491	0.074

Table 2. UBL (in N), UBD (in μm), E (in GPa) and MOR (in GPa) for alternate and longitudinal osteons whose haversian canal was 50 μm in diameter. E was calculated for loads of 0.58 N (E1) and 1.99 N (E2), respectively

	Alternate osteons					Longitudinal osteons				
	UBL	UBD	E1	E2	MOR	UBSg	UBSn	E1	E2	MOR
	1.76	90.5	1.38	(*)	0.24	3.17	139.0	1.84	0.73	0.43
	2.35	74.0	4.43	1.01	0.32	2.94	145.5	1.23	0.36	0.40
	1.88	84.0	3.69	(*)	0.25	2.94	141.9	0.92	0.32	0.40
	2.11	101.5	0.71	0.48	0.29	2.23	266.0	1.23	0.20	0.30
	2.46	116.2	1.63	0.77	0.33	3.05	144.5	2.01	0.50	0.42
	1.99	95.0	0.51	0.39	0.27	2.82	138.0	0.92	0.53	0.38
	3.29	90.0	3.16	1.63	0.45	2.23	136.0	1.38	0.31	0.30
	2.82	60.0	3.69	2.03	0.38	2.23	179.5	1.58	0.24	0.30
	2.58	72.5	1.84	1.21	0.35	2.11	72.0	2.77	0.58	0.29
	2.70	67.0	2.21	1.67	0.37	2.35	70.0	3.69	0.71	0.32
	3.41	70.5	2.21	1.79	0.47	3.29	62.5	4.43	0.93	0.45
						2.58	84.0	4.43	0.87	0.35
						2.23	179.0	2.77	0.28	0.30
						3.17	71.0	3.16	1.93	0.43
Mean	2.48	83.74	2.31	1.22	0.338	2.66	130.64	2.31	0.60	0.362
S.D.	0.54	16.79	1.28	0.59	0.075	0.42	56.21	1.23	0.44	0.059

* Osteons broken before the load of 1.99 N was reached.

compared for each osteonic type (longitudinal and alternate) of the same series, i.e. osteons with a haversian canal measuring 40 μm in diameter, as reported in Tables 3 and 4.

Due to the unusual specimen shape, it is worth emphasizing that the absolute values directly measured or calculated are not so important as the difference between the two types of osteons.

Fractures produced by bending differ substantially according to the type of lamellar structure of osteons. In units having a marked longitudinal spiral course in successive lamellae the fractures normally occur only on the tension side of the central part of the sample, while the compression side appears free (or almost free) of discontinuities [Fig. 1(d)]. In alternate osteons, fractures may appear as a complete interruption of the sample and seem to correspond to quickly traveling cracks [Fig. 1(e)]. Lastly, in both osteon

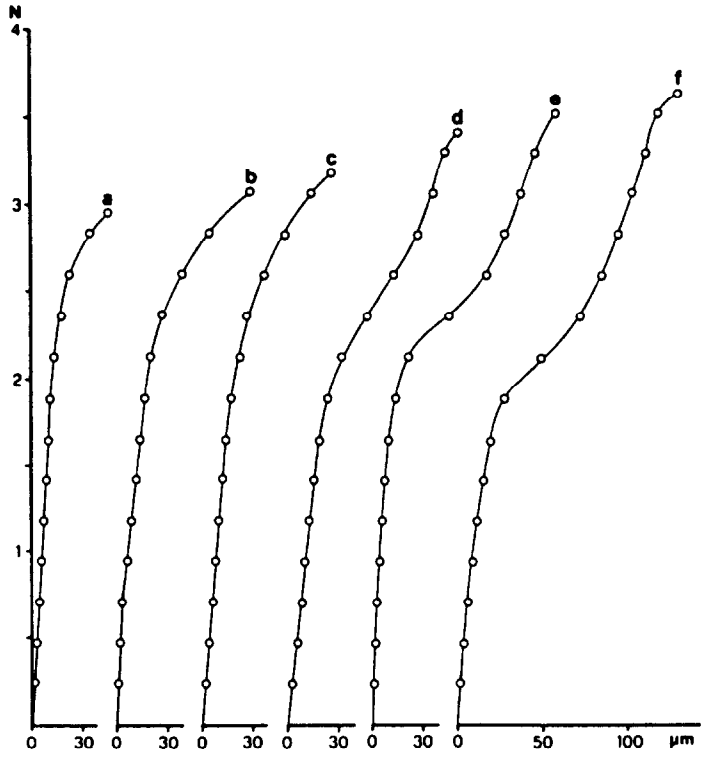

Fig. 3. Load vs deformation curves of three alternate osteons (a, b, c) and three longitudinal osteons (d, e, f), all with a haversian canal measuring 40 μm in diameter and all loaded by bending. Only half of the recorded points have been reported.

Table 3. *P* calculated for pairs of the mean values reported in Table 1 and obtained from longitudinal (L) and alternate (A) osteons (O) with a haversian canal measuring 40 μm in diameter

O	UBL	UBD	E1	E2	MOR
L	2.91 ± 0.47	132.75 ± 30.53	2.32 ± 1.20	0.809 ± 0.491	0.398 ± 0.074
A	2.61 ± 0.38	66.01 ± 17.65	2.69 ± 0.93	1.530 ± 0.79	0.355 ± 0.051
	$P > 0.1$	$P < 0.001$	$P > 0.1$	$P < 0.01$	$0.1 > P > 0.05$

Table 4. *P* calculated for pairs of the mean values reported in Table 2 and obtained from longitudinal (L) and alternate (A) osteons (O) with a haversian canal measuring 50 μm in diameter

O	UBL	UBD	E1	E2	MOR
L	2.66 ± 0.42	130.64 ± 56.21	2.31 ± 1.23	0.60 ± 0.44	0.362 ± 0.059
A	2.48 ± 0.54	83.74 ± 16.19	2.31 ± 1.28	1.22 ± 0.59	0.338 ± 0.075
	$P > 0.1$	$P < 0.02$	$P > 0.1$	$P < 0.01$	$P > 0.1$

types breakage sometimes involves an irregular longitudinal dissociation of the interrupted lamellae [Fig. 1(f)].

DISCUSSION AND CONCLUSION

The first subject of discussion raised by the present investigation is the deformation of osteon samples before ultimate bending strength is reached. When fully calcified osteons are considered, those consisting of longitudinal lamellae bend easily, while those consisting of alternate lamellae show little deformation by bending. Such findings can be examined more analytically when the two different types of load–deformation curves recorded from longitudinal and alternate osteons are compared. Since the features of the diagrams for the two osteon series can best be understood on a comparative basis, this topic will be discussed globally.

The curves recorded from longitudinal osteons are

somewhat composite. Initially they approximate to a straight line after which there is an early elasto–plastic flection. This is followed by a new straightening. The curves obtained from alternate osteons reveal a long straight line. Only the uppermost points show an elasto–plastic flection line before the breaking point is reached.

To explain these differences in the behaviour of the two osteon types, it seems appropriate to recall that, in alternate osteons, the lamellae whose collagen fiber bundles and crystallites have a transversal course function as rings or cylinders which interfere with the flexibility of the lamellae whose collagen fiber bundles and crystallites have a longitudinal course. So, when the proportional limit is reached and the lamellae whose collagen fibers and crystallites have a transversal course give way, the remaining lamellae, whose collagen fibers and crystallites have a longitudinal course, are no longer able to support an increasing load.

In longitudinal osteons, lamellae whose fibers and crystallites have a transversal course are reduced to thin, incomplete arches. So when these structures begin to give way and early plastic deviation occurs, many longitudinal fibers and crystallites are left; these are able to support additional loads. This accounts for the straightening of the curve observed in the diagram.

The results conveyed by the diagrams are again fully in line with expectations when the numerical data are considered.

In spite of the circumstance that in longitudinal osteons the fibers and crystallites with a transversal course are no more than thin, incomplete arches, the elastic modulus is not significantly different for the initial portion of the curves recorded from the two osteon types. This means that the thin transverse components are able to provide longitudinal osteons with an initial compactness. As the load increases, however, the longitudinal osteons show a significant fall in their elastic modulus, with plastic deformation, and this is not compensated for by the straightening in the terminal portion of the diagram. In fact the ultimate bending strain is significantly higher in longitudinal than in alternate osteons. In spite of the differences in the behaviour of the diagrams recorded from the two osteon types, the higher ultimate bending strength shown by longitudinal osteons does not seem to be statistically significant.

Summing up, from all the results discussed above, it may be inferred that longitudinal osteons are less able to withstand loading by bending than alternate osteons, on account of their earlier elasto–plastic deformation.

When the load–deformation curves obtained from osteon samples are compared with the load–deformation curves recorded from an entire femur at macroscopic level, some differences become apparent. According to Martens *et al.* (1986), the load vs deformation curve for a femoral bone structure which fails at the middle, i.e. at the point of maximum bending, demonstrates a considerable zone of non-linearity prior to failure. On the other hand, the load vs deformation curve for a femur which fails at the distal third, i.e. beyond the point where the load is directly applied, fails to show any plastic portion. Of these two types of load–deformation curves, only that revealing a zone of non-linearity prior to failure was recorded for all the osteons tested.

The shape of fractures in the middle region of tested osteon specimens differed according to osteon type. In longitudinal osteons, lamellae normally failed only on the tension side. In alternate osteons, however, cross-fracture usually led to breakage of the whole width of the sample in its middle region. Longitudinal discontinuities giving the fracture an irregular shape were observed in both osteon types.

It is not easy to explain how and in what sequence cracks appear in longitudinal and alternate osteon samples loaded by bending. Microscopic examination during loading of the sample is unable to provide reliable results, because the damage is done quickly. At present, any attempt to analyse the phenomenon can only be speculative. As regards longitudinal osteons, an explanation may be offered by taking as a model the mechanism of wood fractures (Kollmann and Côté, 1968). When, during the loading by bending of an osteon sample, the phase of plastic deformation is reached and the ultimate bending stress is approached, strong deformation occurs on the pressure side.

As a result, the neutral line moves toward the tension side, where resistance fails and a fracture occurs. On the other hand, when an alternate osteon sample is loaded by bending, the rigidity induced by transverse lamellae reduces deformation on the pressure side and increases resistance on the tension side, so that as soon as resistance breaks down on the tension side, fracture suddenly occurs and quickly spreads right through the cross-section of the osteon. Lastly, when fracture occurs in a longitudinal direction in either osteon type, it reveals an irregular separation of the broken lamellae. This suggests that, besides the maximum bending moment coming to bear on the middle region of the osteon, shear force may be critical, causing fracture at a point with a lower bending moment.

In conclusion, the fact that alternate osteons contain transverse lamellae accounts for their greater rigidity with respect to longitudinal osteons. It is, therefore, only to be expected that the incidence of alternate osteons in bowed bones should be very high, since their presence there will help to forestall any worsening of the deformation (Ascenzi *et al.*, 1987).

Acknowledgements—The present study has been supported by grants Nos 85.00662.04 and 86.00424.04 from the National Research Council of Italy.

The authors are grateful to Mr. L. Virgilii for his valuable assistance in preparing the photographic material.

REFERENCES

Ascenzi, A. (1983) Microscopic dissection and isolation of bone constituents. *Skeletal Research, An Experimental Approach* (Edited by Kunin, A. S. and Simmons, D. J.), Vol. 2, pp. 185–236. Academic Press, New York.

Ascenzi, A. and Benvenuti, A. (1986) Orientation of collagen fibers at the boundary between two successive osteonic lamellae and its mechanical interpretation. *J. Biomechanics* **19**, 455–463.

Ascenzi, A., Benvenuti, A., Mango, F. and Simili, R. (1985) Mechanical hysteresis loops from single osteons: technical devices and preliminary results. *J. Biomechanics* **18**, 391–398.

Ascenzi, A. and Bonucci, E. (1967) The tensile properties of single osteons. *Anat. Rec.* **158**, 375–386.

Ascenzi, A. and Bonucci, E. (1968) The compressive properties of single osteons. *Anat. Rec.* **161**, 377–391.

Ascenzi, A. and Bonucci, E. (1976) Relationship between ultra-structure and 'Pin Test' in osteons. *Clin. Orthop. Rel. Res.* **121**, 275–294.

Ascenzi, A., Bonucci, E. and Checcucci, A. (1966) The tensile properties of single osteons studied using a microwave extensimeter. *Studies on the Anatomy and Function of Bone and Joints* (Edited by Evans, F. G.), pp. 121–141. Springer, Berlin.

Ascenzi, A., Boyde, A., Portigliatti Barbos, M. and Carando, S. (1987) Micro-biomechanics vs macro-biomechanics in cortical bone. A micro-mechanical investigation of femurs deformed by bending. *J. Biomechanics* **20**, 1045–1053.

Azang, E., Posch, P. and Engelbracht, R. (1972) Experimentelle Untersuchungen über die Bruchfestigkeit des menschlichen Schienbein. *Wschr. Unfallheilk.* **25**, 336–344.

Ehler, E. and Lösche, H. (1970) Biegeversuche am menschlichen Femur. *Beitr. orthop. Traumatol.* **17**, 304–314.

Evans, F. G. (1973) *Mechanical Properties of Bone*. Thomas, Springfield, Illinois.

Giraud-Guille, M. M. (1988) Twisted plywood architecture of collagen fibrils in human compact bone osteons. *Calcif. Tissue Int.* **42**, 167–180.

Knese, K. H., Hahne, O. and Biermann, H. (1956) Festigkeitsuntersuchungen an menschlichen Extremitätenknochen. *Gegenbaur morph. Jb.* **96**, 141–209.

Kollmann, F. F. P. and Côté, W. A. Jr (1968) *Principles of Wood Science and Technology*. Springer, Berlin.

Maj, G. (1938a) Resistenza meccanica del tessuto osseo a diversi livelli di uno stesso osso. *Boll. Soc. ital. Biol. sper.* **13**, 413–415.

Maj, G. (1938b) Osservazioni sulle differenze topografiche della resistenza meccanica del tessuto osseo di uno stesso segmento scheletrico. *Monitore zool. ital.* **49**, 139–149.

Maj, G. and Toajari, E. (1937) Osservazioni sperimentali sul meccanismo di resistenza del tessuto osseo lamellare compatto alle azioni meccaniche. *Chir. Org. Mov.* **22**, 541–557.

Martens, M., Audekercke, R. van, Meester, P. de and Mulier, J. C. (1986) Mechanical behaviour of femoral bones in bending loading. *J. Biomechanics* **19**, 443–454.

Mather, B. S. (1968) Variation with age and sex in strength of the femur. *Med. Biol. Engng* **6**, 129–132.

Messerer, O. (1880) *Ueber Elasticität und Festigkeit der menschlichen Knochen*. Gottaschen, Stuttgart.

Motoshima, T. (1960) Studies on the strength for bending bony extremity bones. *J. Kyoto Pref. Univ. Med.* **68**, 1377–1397.

Olivo, O. M. (1937) Rispondenza della funzione meccanica varia degli osteoni con la loro diversa minuta architettura. *Boll. Soc. ital. Biol. sper.* **12**, 400–401.

Olivo, O. M., Maj, G. and Toajari, E. (1937) Sul significato della minuta struttura del tessuto osseo compatto. *Boll. Sci. Med.* **109**, 369–394.

Rauber, A. A. (1876) *Elasticität und Festigkeit der Knochen*. Engelmann, Leipzig.

Sedlin, E. D. (1965) A rheological model for cortical bone. *Acta orthop. scand.* **83** (suppl.).

Stevens, J. and Ray, R. D. (1962) An experimental comparison of living and dead bone in rats. Physical properties. *J. Bone Jt Surg.* **44B**, 412–423.

Toajari, E. (1938) Resistenza meccanica ed elasticità del tessuto osseo studiata in rapporto alla minuta struttura. *Monitore zool. ital.* **48**, 148–154.

Yamada, H. (1970) *Strength of Biological Materials* (Edited by Evans, F. G.). Williams and Wilkins, Baltimore.